Tumor induction by disruption of the Dnmt1, PCNA and UHRF1 interactions.

Eric Hervouet[1-2], Lisenn Lalier[1-2], Emilie Debien[1-2], Mathilde Cheray[1-2], Audrey Geairon[3], Hélène Rogniaux[3], François M. Vallette[1-2] and Pierre-François Cartron[1-2*].

[1] INSERM, U892, Equipe Apoptose et progression tumorale, Equipe labellisée Ligue Nationale Contre le Cancer. F-44000, Nantes, France.

[2] Université de Nantes, Faculté de Médecine, Département de Recherche en Cancérologie, IFR26, F-4400, Nantes, France.

[3] INRA UR1268 Biopolymère Interactions Assemblages, Plate-Forme BIBS, F-44300 Nantes, France

[*] correspondance should be addressed to pierre-francois.cartron@univ-nantes.fr

The low level of DNA methylation in tumors compared to the level of DNA methylation in their normal-tissue counterparts or global DNA hypomethylation was one of the first epigenetic alterations to be found in human cancer[1, 2]. While the contribution of genome hypomethylation in cancer development and progression is explained by several mechanisms: chromosomal instability, loss of imprinting, and reactivation of transposable elements[3, 4], the molecular causes of genome hypomethylation remain unclear. Indeed, despite the central roles of the DNA methyltransferases (Dnmts) in the establishment and maintenance of the DNA methylation, no clear consensus appears between the reduction of the Dnmts expression and the genome hypomethylation in human cancers[5]. Nevertheless, the cancer-associated genome hypomethylation could be explained by the disruption of interactions existing between Dnmts and the DNA replication and DNA repair proteins because these interactions play a crucial role in the DNA methylation in mammalian cells[6-8]. We here demonstrate that the disruption of the Dnmt1/PCNA and Dnmt1/UHRF1 interactions induce the genome hypomethylation and act as oncogenic factors promoting the tumorigenesis. We also identify the Akt- and/or PKC-mediated phosphorylations of Dnmt1 as both initiators of these disruptions and as a hallmark conferring poor prognosis in glioma patients.

The global DNA methylation status of gliomas was assessed by measuring the number of 5-methylcytosine (5mC) in a collection of 62 surgical resections of gliomas and in 5 non-pathologic brain biopsies (**Figure 1a**). ELISA results indicate that the 5mC number decreases when the glioma grade increases (Pearson's correlation test, r=-0.504, p<0.0001). We next complemented this observation by measuring the intra-tumor *de novo* and maintenance DNA methyltransferase activities (dnMTase and mMTase) in order to determine the contribution of each MTase activities on the global DNA hypomethylation phenotype characterizing the gliomagenesis. Each MTase activity was plotted against the 5mC data and a statistical analysis using the Pearson's correlation test showed a significant correlation between the 5mC and the mMTase activity (r=0.760, p<0.0001), but not between the 5mC and the dnMTase activity (r=0.135, p=0.2761) (**Figure 1b**). The Dnmt1 being the predominant maintenance methyltransferase enzyme, we next assessed its expression in glioma biopsies by ELISA. No significant correlation was observed between the Dnmt1 expression and the mMTase activity (Pearson's correlation test, r=-0.202, p=0.1012) (**Figure 1c**). Gliomagenesis involving a stepwise accumulation of kinases, we decided to determinate whether the Dnmt1 phosphorylation was a molecular determinant governing the mMTase activity decrease seen above. For this purpose, we estimated the amount of phosphorylated Dnmt1 (pDnmt1) by ELISA using a panel of motif specific antibodies (phospho-Akt substrate-specific (PAS), phospho-(ser)-PKC substrate (PPCS), phospho-(thr)- and phospho-(ser)-CDK substrate (PCS)). pDnmt1-PAS, pDnmt1-PPCS, and pDnmt1-PCS values were plotted against the mMTase activity values. Significant inverse correlations were observed between the pDnmt1-PAS or the pDnmt1-PPCS levels and the mMTase activity (Pearson's correlation test, r=-0.569, p<0.0001 and r=-0.454, p=0.0001), but not between the pDnmt1-PCS and the mMTase activity (Pearson's correlation test, r=-0.045, p=0.7177) (**Figures 1d and S1**).

We next analyzed whether the presence of high quantities of both pDnmt1-PAS and pDnmt1-PPCS could affect the survival time of a subgroup of 53 glioma patients for which we obtained a well-documented medical history (**Table S1**). Based on the pDnmt1-PAS and pDnmt1-PPCS levels found on tumor biopsies, the 53 patients were divided into two groups. 18 patients whose tumors expressed high levels of pDnmt1-PAS and pDnmt1-PPCS simultaneously (equal to or higher than the median value of considered grade) were included in group#1 (in grey on table S1), while 35 patients whose tumors are devoid of this hallmark composed the group#2. Survival curves were estimated by the Kaplan-Meier method and compared with the Cox proportional hazards survival regression test (**Figure 1e**). Thus, we observed a significant difference in survival time between patients whose tumors had a high

pDnmt1-PAS and pDnmt1-PPCS levels and those whose did not (p=0.001). These results indicate that the high presence of Akt- and PKC-phosphorylated forms of Dnmt1 could be used as an alternative molecular biomarker to predict the disease outcome and/or the prognosis of glioma.

To assess the impact of the Akt- and PKC-phosphorylations of Dnmt1 on the functionality of this enzyme in glioma cells with characteristics similar to the cells present in the tumor mass, we next decided to extend our analyses to primary cultured tumor cells (PCTC) obtained from gliomas because established cell lines diverged from original cells[9]. ELISA, DMB assay and immunoblots confirmed that PCTCs (as tumors) are characterized by a decrease of 5mC number, a diminution of the mMTase activity, and an increase of the pDnmt1-PAS and/or pDnmt1-PPCS levels all the more important that the tumor grade is elevated (**Figure 2a**). Bisulfite sequencing and Chromatin ImmunoPrecipitation (ChIP) corroborated these points by showing that the Alu methylation status and the Dnmt1 recruitment on this DNA repeat element decreased when the tumor grade increased (**Figure 2b**). Consistent with these results, we then characterized the Akt- or PKC-mediated phosphorylations of recombinant human Dnmt1 (rh-Dnmt1). Mass spectrometric analyses indicated that Akt phosphorylated rh-Dnmt1 at serine-127 and 143 while PKC phosphorylated rh-Dnmt1 at serine-127 (**Figure 2c and S2**). Strikingly, it appears that these phosphorylations are included within or juxtapose the interaction domains of Dnmt1 with PCNA and UHRF1 identified by Chuang et al. (1997)[7] and Bostick et al. (2007)[6]. Thus, we hypothesized that the Akt- and PKC-induced Dnmt1 phosphorylations could act as two molecular determinants inhibiting the Dnmt1 recruitment on DNA via the disruption of the Dnmt1/PCNA and Dnmt1/UHRF1 interactions because PCNA and UHRF1 proteins mediating the epigenetic inheritance in mammalian cells by recruiting Dnmt1[6, 8]. This idea was first demonstrated by the fact that the Akt and/or PKC-induced phosphorylations of rh-Dnmt1 inhibited the Dnmt1/PCNA and/or Dnmt1/UHRF1 interactions in pull down assay, but not the Dnmt1/HDAC1 interaction (**Figure 2d**). Secondly, our hypothesis was validated by the fact that the amount of Dnmt1/PCNA and Dnmt1/UHRF1 interactions is (supprimé) correlated with the level of Dnmt1 recruited on DNA (**Figure 2e**). Thirdly, the fact that Akt and PKC inhibitor treatments restored the Dnmt1/PCNA and Dnmt1/UHRF1 interactions in PCTCs also supported the idea that the Akt- and PKC-induced Dnmt1 phosphorylations negatively regulated the Dnmt1/PCNA and Dnmt1/UHRF1 interactions (**Figure 2f**). Thus, all these results demonstrate that the decrease of both Dnmt1/PCNA and Dnmt1/UHRF1 interactions for the benefit of the presence of pDnmt1-PAS and pDnmt1-PPCS is a crucial molecular

event generating the decrease of 5mC number seen in tumors via the decrease of mMTase activities. This last point was demonstrated by DMB assay and the hierarchical classification of the mMTase activity effectors namely Dnmt1, pDnmt1-PAS, pDnmt1-PPCS, Dnmt1/PCNA and Dnmt1/UHRF1. Indeed, we noted that the Dnmt1/PCNA and Dnmt1/UHRF1 dimers catalyzed 5-fold more incorporation of methyl group ^{3}H-radiolabelled than pDnmt1-PAS and pDnmt1-PPCS, and 20-fold more incorporation of methyl group ^{3}H-radiolabelled than the Dnmt1 (**Figure 2g**). In summary, our data identify Akt- and PKC-induced phosphorylations of Dnmt1 as the initiators of the disruption of the Dnmt1/PCNA and Dnmt1/UHRF1 interactions, and the switch "Dnmt1/PCNA and Dnmt1/UHRF1 to pDnmt1-PAS and pDnmt1-PPCS" as the effector of the global DNA hypomethylation phenotype seen in tumors.

We finally wondered whether the global DNA hypomethylation generated disruption of Dnmt1/PCNA and Dnmt1/UHRF1 interactions was an event able to transform the Ntv-a glial cells into glioma. For this purpose, we designed the peGFP-UP plasmid expressing the chimerical protein composed by the GFP reporter protein and by the U and P peptides (defined figure 2c), whose expression inhibited the Dnmt1/PCNA and Dnmt1/UHRF1 interactions but not the Dnmt1/HDAC1 interaction in pull down assay (**Figure S3**). ELISA and immunoprecipitation showed that the Ntv-a/peGFP-UP cells harbored a low level of 5mC via the disruption of the Dnmt1/PCNA and Dnmt1/UHRF1 interactions, compared to the Ntv-a/peGFP cells (**Figure 3a**). The tumorogenicity of the Ntv-a/peGFP-UP and Ntv-a/peGFP cells was assessed by s.c. injection into nude mice and was compared to that of the Ntv-a/PDGF and Ntv-a/RasAkt cells obtained from the experimental RCAS-system of gliomagenesis[10, 11]. After 2 weeks, we observed macroscopically visible tumors in all 26 injections of Ntv-a/peGFP-UP cells (**Figure 3b**). The growth pattern of Ntv-a/peGFP-UP-induced tumors was similar to that of the tumors formed from the injection of Ntv-a/Ras-Akt cells. We also noted that 4/26 Ntv-a/peGFP-UP-induced tumors were invasive (**Figure S4**). In culture, the Ntv-a/peGFP-UP cells harbored several hallmarks of cancer cells namely apoptosis evasion, high clonogenicity and high proliferation rate (**Figure 3c**). At molecular level, we observed that the Ntv-a/peGFP-UP cells were characterized by the hypomethylation-induced overexpression of BDNF and PDGF-B (**Figures 3d and S5**). These findings confirm that the BDNF and PDGF-B genes are epigenetically regulated[12, 13] and suggest that the Ntv-a/peGFP-UP cells acquire the cancer hallmark of self-sufficiency in growth signals[14]. Taken together these results strongly demonstrate that the disruption of the Dnmt1/PCNA and Dnmt1/UHRF1 interactions acts as an oncogenic factor because this event

induces the *in vivo* tumorogenicity, the acquisition of 3 cancer hallmarks[14] (i.e. apoptosis evasion, high proliferation and self-sufficiency in growth signals) and the overexpression of PDGF-B, an oncogene clearly implicated in gliomagenesis[10, 15, 16] (**Figure 4**). Thus, while several papers demonstrate that PCNA and/or UHRF1 play a crucial role in the recruitment and/or the anchorage of Dnmt1 on DNA to maintain the DNA methylation pattern of mammalian cells via the capacity of these proteins to bind DNA and hemi-methylated DNA[6, 8, 17-19], our work is one of the first to identify the disruption of Dnmt1, PCNA and UHRF1 interactions as a crucial molecular determinant governing the global DNA hypomethylation occurring in tumors. Despite the undoubted role of the chromosomal instability induced by the global DNA hypomethylation in the tumorogenesis[20, 21], our data suggest that the gene-specific hypomethylation of oncogenes (like PDGF-B) could be an alternative mechanism contributing to the hypomethylation-induced tumor. Due to its oncogenic role, the identification of molecular mechanisms governing the Dnmt1, PCNA and UHRF1 interactions provides new potential therapeutic targets and reinforces the interest to investigate the use of Akt and/or PKC inhibitors in the design of anti-glioma therapeutic protocols.

METHODS SUMMARY

ELISA.

Microtiter plate was coated with capture antibody (anti-Dnmt1, Santa Cruz sc-10221, 2µg/ml in 100µl of coating buffer) for overnight at 4°C. After 3 washes in PBS/Tween buffer (PBS pH 7.2-7.4, Tween-20, 0.05%), microtiter plate was blocked with 200µl /well of blocking buffer (PBS pH 7.2, 10% Fetal calf serum) for 30min at room temperature. After 3 washes in PBS/Tween buffer, samples are incubated for overnight at 4°C. After 3 washes in PBS/Tween buffer, detection antibody (Cell Signaling, Ozyme France) is incubated at the concentration of 2 µg/ml in 100µl blocking buffer for 1h at room temperature. Revelation is performed by inbucating 50 µl/well of alkaline phosphatase conjugated secondary antibody diluted to 1:500 in blocking buffer at room temperature for 1h. Wells are then washed three times with PBS/Tween buffer and once with diethanolamine buffer (10 mM diethanolamine, 0.5 mM $MgCl_2$ (pH 9.5) prior to pNPP substrate (Santa Cruz) addition in diethanolamine buffer to a final concentration of 1 mg/ml. Reaction is stopped by adding 0.1M EDTA and read on microtiter plate reader at OD 405/490.

DNA methylation analyses.

DNA was extracted by using the QiaAmp DNA mini Kit (Qiagen, France) and bisulfite conversion was realized by using the EZ DNA methylation Gold kit (Zymo Research – Proteigene, France) according to manufacturer's instructions. Sequencing of bisulfite-modified DNA was performed on 25 clones generated in two to three independent bisulfite modifications. Methylation status of PDGF-B and BDNF were analyzed by Methylation Sensitive Restriction Assay (MSRA) and Methylation Specific PCR (MSP) according to the primers design by using the MethPrimer program (**Figure S4**).

Tumorogenicity assay.

Cultured cells were harvested by trypsinization, washed and resuspended in saline buffer. Cell suspensions were injected s.c. as 10^6 cells in 0.2 ml volume in the flank of 7/8-week-old Nude NMRI-nu female mice (Janvier, France). Mice were checked for tumor onset and tumor growth twice a week. Tumor parameters were measured by a caliper, and the tumor volumes were calculated by multiplying them.

Preparation of Ntv-a/peGFP-UP cells.

Ntv-a cells come from the laboratory of Eric C. Holland (Memorial Sloan Kettering Cancer Center, New York). The peGFP-UP was obtained by subcloning the sequences coding for the U and P peptides (defined figure 2c) into the BglII/SacII sites of the peGFP-N plasmid (Clontech, France). Ntv-a/peGFP-UP cells were obtained after nucleofection by using the Mouse Astrocyte Nucleofector™ kit (Amaxa biosystems, France) according to the manufacturer's instructions.

Statistical Analysis.

According to the internal committee of bioethics, the overall survival time was measured from the date of surgical resection to the last follow-up visit or death. Patients with tumor recurrence or partial resection or a Karnofsky Performance Index inferior to 80 were censored. Data in bar graphs are expressed as the mean±SD. Each result is representative of three independent experiments.

Author contributions

P.F.C., F.M.V. and E.H. designed the study. All experiments involving mice were performed by E.D. P.F.C., M.C. and E.H. carried out the IP, ChIP, western blot, pull-down and ELISA

analyses. E.H. constructed the peGFP-UP plasmid and carried out all experiments realized with the Ntv-a/peGFP and Ntv-a/peGFP-UP cells. L.L., A.G. and H.R. carried out the mass spectrometric analyses and were involved in interpretation of results. All authors discussed the results and commented on the manuscript written by P.F.C.

REFERENCES.

1. Gama-Sosa, M. et al. The 5-methylcytosine content of DNA from human tumors. Nucleic Acids Res 11, 6883-94 (1983).

2. Feinberg, A. & Vogelstein, B. Hypomethylation distinguishes genes of some human cancers from their normal counterparts. Nature 301, 89-92 (1983).

3. Esteller, M. Epigenetics in cancer. N Engl J Med. 358, 1148-59 (2008).

4. Hoffmann, M. & Schulz, W. Causes and consequences of DNA hypomethylation in human cancer. Biochem Cell Biol. 83, 296-321 (2005).

5. Ehrlich, M. et al. Quantitative analysis of associations between DNA hypermethylation, hypomethylation, and DNMT RNA levels in ovarian tumors. Oncogene 25, 2636-45 (2006).

6. Bostick, M. et al. UHRF1 plays a role in maintaining DNA methylation in mammalian cells. Science 27, 2187-97 (2007).

7. Chuang, L. S. et al. Human DNA-(cytosine-5) methyltransferase-PCNA complex as a target for p21WAF1. Science. 277, 1996-2000 (1997).

8. Sharif, J. et al. The SRA protein Np95 mediates epigenetic inheritance by recruiting Dnmt1 to methylated DNA. Nature 450, 908-12 (2007).

9.   Lee, J. et al. Tumor stem cells derived from glioblastomas cultured in bFGF and EGF more closely mirror the phenotype and genotype of primary tumors than do serum-cultured cell lines. Cancer Cell 9, 391-403 (2006).

10.   Dai, C. et al. PDGF autocrine stimulation dedifferentiates cultured astrocytes and induces oligodendrogliomas and oligoastrocytomas from neural progenitors and astrocytes in vivo. Genes Dev. 15, 1913-25 (2001).

11.   Holland, E. C. Gliomagenesis: genetic alterations and mouse models. Nat Rev Genet. 2, 120-9 (2001).

12.   Martinowich, K. et al. DNA methylation-related chromatin remodeling in activity-dependent BDNF gene regulation. Science 302, 890-3 (2003).

13.   Bruna, A. et al. High TGFbeta-Smad activity confers poor prognosis in glioma patients and promotes cell proliferation depending on the methylation of the PDGF-B gene. Cancer Cell 11, 147-60 (2007).

14.   Hanahan, D. & Weinberg, R. The hallmarks of cancer. Cell 100, 57-70 (2000).

15.   Shih, A. & Holland, E. Platelet-derived growth factor (PDGF) and glial tumorigenesis. Cancer Lett. 232, 139-47 (2006).

16.   Westermark, B., Heldin, C. & Nistér, M. Platelet-derived growth factor in human glioma. Glia 15, 257-63 (1995).

17.   Arita, K., Ariyoshi, M., Tochio, H., Nakamura, Y. & Shirakawa, M. Recognition of hemi-methylated DNA by the SRA protein UHRF1 by a base-flipping mechanism. Nature Epub ahead of print (2008).

18.   Avvakumov, G. et al. Structural basis for recognition of hemi-methylated DNA by the SRA domain of human UHRF1. Nature Epub ahead of print (2008).

19.   Hashimoto, H. et al. The SRA domain of UHRF1 flips 5-methylcytosine out of the DNA helix. Nature Epub ahead of print (2008).

20.   Eden, A., Gaudet, F., Waghmare, A. & Jaenisch, R. Chromosomal instability and tumors promoted by DNA hypomethylation. Science. 300, 455 (2003).

21.   Gaudet, F. et al. Induction of tumors in mice by genomic hypomethylation. Science. 300, 489-92 (2003).

22.   Yokochi, T. & Robertson, K. D. DMB (DNMT-magnetic beads) assay: measuring DNA methyltransferase activity in vitro. Methods Mol Biol. 287, 285-96 (2004).

23.   Fuks, F., Burgers, W. A., Brehm, A., Hughes-Davies, L. & Kouzarides, T. DNA methyltransferase Dnmt1 associates with histone deacetylase activity. Nat Genet. 24, 88-91 (2000).

24. Achour, M. et al. The interaction of the SRA domain of ICBP90 with a novel domain of DNMT1 is involved in the regulation of VEGF gene expression. Oncogene 27, 2187-97 (2008).

25. Cartron, P. F. et al. Nonredundant role of Bax and Bak in Bid-mediated apoptosis. Mol Cell Biol 23, 4701-12 (2003).

LEGENDS.

Figure 1. Presence of high levels of Akt- and PKC-induced phosphorylations of Dnmt1 confers poor prognosis in glioma patients.

a, Correlation between the 5-methylcytosine number (5mC) and tumor grade in a collection of 67 DNA samples including 16 grade II astrocytomas/oligodendrogliomas, 16 grade III astrocytomas/oligodendrogliomas, 30 grade IV astrocytomas/GBM and of 5 non-tumor brain samples (nt). 5mC was estimated by using the Methylamp Global DNA Methylation Quantification kit (Epigentek-Euromedex, France). Dotted lines represent the median of each parameter.

b, Correlation study between the 5-methylcytosine number (5mC) and the *de novo* (supprimé) methyltransferase (dnMTase) or the maintenance methyltransferase (mMTase) activities. Intra-tumor mMTase and dnMTase activities were calculated by using hemi-methylated and unmethylated DNA substrates in DMB assays according to Yokochi and Robertson (2004)[22]. ◇ represents nt, ☐ represents grade II astrocytomas/oligodendrogliomas, △ represents grade III astrocytomas/oligodendrogliomas, O represents grade IV astrocytomas/GBM.

c, Correlation study between relative Dnmt1 expression and the mMTase activity. The relative Dnmt1 expression was assessed by using the EpiQuick Dnmt1 assay (Epigentek-Euromedex, France). ◇ represents nt, ☐ represents grade II astrocytomas/oligodendrogliomas, △ represents grade III astrocytomas/oligodendrogliomas, O represents grade IV astrocytomas/GBM.

d, Correlation study between the mMTase activity and the fraction of Dnmt1 recognized by a specific antibody detecting the phospho-Akt substrate (pDnmt1-PAS) and the phospho-PKC substrate (pDnmt1-PPCS) (Cell Signaling). ◇ represents nt, ☐ represents grade II astrocytomas/oligodendrogliomas, △ represents grade III astrocytomas/oligodendrogliomas, O represents grade IV astrocytomas/GBM.

e, Kaplan-Meier estimates time of survival between patients suffering from glioma presenting a high level of both pDnmt1-PAS and pDnmt1-PPCS (grey line) and those whose tumors did not (black line).

Figure 2. The Akt- and/or PKC-induced phosphorylations of Dnmt1 disrupt the Dnmt1/PCNA and Dnmt1/UHRF1 interactions.

a, 5-methylcytosine (5mC) number, maintenance methyltransferase (mMTase) activity and level of pDnmt1-PAS and pDnmt1-PPCS in a panel of PCTC issued from the different grade of gliomas. 5mC number was assessed by using the Methylamp Global DNA Methylation Quantification kit (Epigentek-Euromedex, France). mMTase activities were measured according to the method described by Yokochi and Robertson (2004)[21]. Immunoblots were performed from 75µg of proteins and Actin was used as loading control.

b, Parallel between Dnmt1-recruitement on Alu, a DNA repeat element assessed by Chromatin Immunoprecipitation assay (ChIP) and the methylation status of Alu analyzed by bisulfite sequencing. ChIP was performed by using the Chromatin EZ-Chip kit (Millipore, France) with antibodies specific for of Dnmt1 or GFP (control). The average number of methylated CpG is indicated for each glioma grade.

c, Schematic representation of Dnmt1. The structural/functional? domains of Dnmt1 are delimited according to the data given by on Expasy/UniProtKB/Swiss-Prot (accession number P26358) The domains of interaction of Dnmt1 with PCNA (163-174), HDAC1 (686-812) and UHRF1 (1-446, 1081-1408 and/or 401-615) are the ones highlighted by Chuang et al. (1997)[7], Fuks et al. (2000)[23], Bostick et al. (2007)[6] and Achour et al. (2008)[24]. The domain of UHRF1 interacting with Dnmt1 is also indicated consistent with Achour et al. (2008)[23]. Phosphorylated serines highlighted by mass spectrometry analyses are indicated in figure.

d, GST pull-down assay analyzing the interactions between the phosphorylated or not recombinant human His tagged Dnmt1 (rh-Dnmt1-Methylation Ltd, Port Orange, Florida) and GST-UHRF1, GST-HDAC1 or GST-PCNA. All GST pull-down assays were validated by immunoblot analysis with anti-Dnmt1 antibody. i represents a loading control of rh-Dnmt1 and c represents the pull-down realized without GST-fusion protein.

e, Interaction between Dnmt1 and PCNA and/or UHRF1 and chromatin association of Dnmt1. Immunoprecipitations were performed by using the Catch&Release v2.0 reversible immunoprecipitation system (Millipore, France). H3 was used as loading control.

f, Effect of PKC inhibitor (PKC[i] or Gö6893, 0.5µM Calbiochem, France) and Akt inhibitor (Akt[i], 0.1µM-Calbiochem#124005, France) treatments on the Dnmt1/PCNA and Dnmt1/UHRF1 interactions. PCTCs were treated for 5 consecutive days with PKC[i] and Akt[i] previous to perform Dnmt1 immunoprecipitation from chromatin. The phosphorylation status of Dnmt1 was estimated by western blots.

g, Analysis of the maintenance methyltransferase (mMTase) activity catalyzed by different forms of Dnmt1. mMTase activities were assessed by DMB assay according to Yokochi and Robertson (2004)[21].

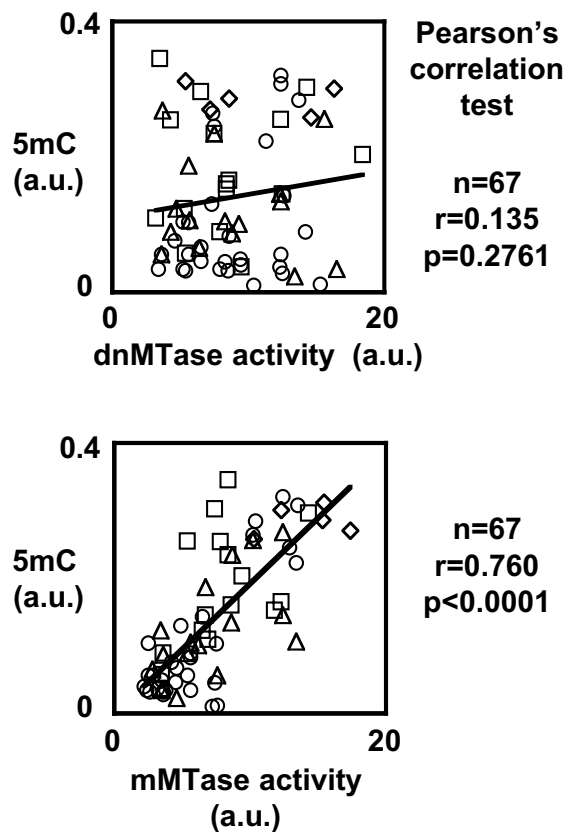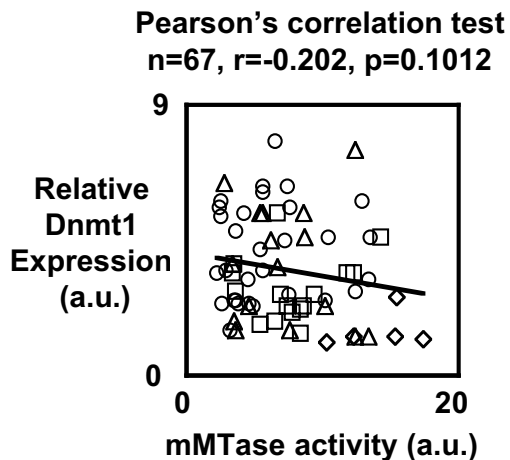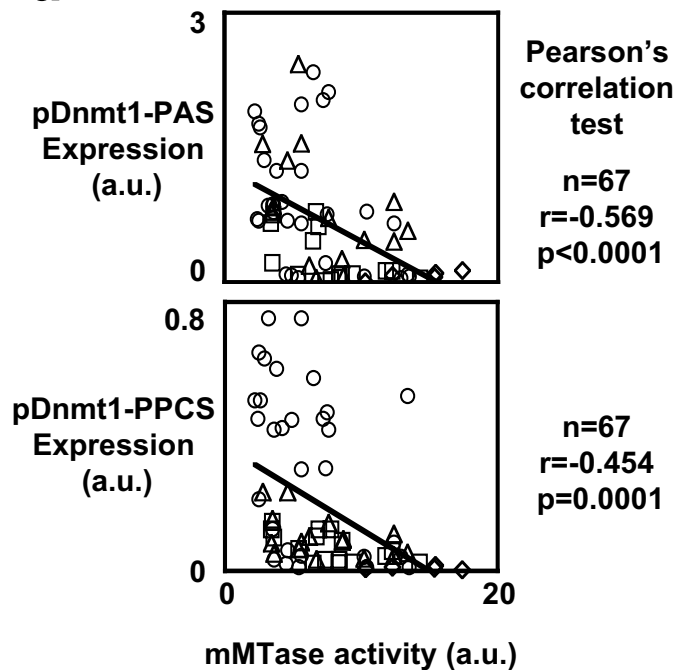## Figure 3. The disruption of the Dnmt1/PCNA and Dnmt1/UHRF1 interactions acts as an oncogenic factor.

a, Impact of the GFP-UP protein expression on Dnmt1/PCNA and Dnmt1/UHRF1 interactions and 5-methylcytosine (5mC) number. These two parameters have been analyzed 15 days after nucleofection of Ntv-a cells by the peGFP-UP and peGFP plasmids.

b, Tumorogenicity test of the Ntv-a/peGFP-UP cells. Graph represents the tumor volumes obtained after s.c injection of nude mice with Ntv-a/peGFP-UP cells (26 injections), Ntv-a/peGFP cells (12 injections), Ntv-a/PDGF cells (8 injections) and Ntv-a/Ras-Akt cells (8 injections). Photographs illustrate the results of a representative injection of Ntv-a/peGFP (left) and Ntv-a/peGFP-UP (right) cells (left), of the *in situ* absence of Ntv-a/peGFP-induced tumor cells (middle-top) and of the *in situ* presence of Ntv-a/peGFP-UP-induced tumors (middle-bottom), and the mean volume of Ntv-a/peGFP-UP-induced tumor cells (right-top), Ntv-a/PDGF-induced tumor cells (right-middle) and Ntv-a/Ras-Akt-induced tumor cells (right-bottom).

c, Comparison of the apopto-sensitivity (via the measure of DEVDase activity), proliferation rate (via the measure of Ki67 expression) and of the clonogenicity index between the Ntv-a/peGFP and Ntv-a/peGFP-UP cells. DEVDase activity and clonogenicity have been assessed as previously described[25]. Relative Ki67 expression was evaluated by sqPCR (s: GACAGCTTCCAAAGCTCACC and as: TGTGTCCTTAGCTGCCTCCT).

d, Correlation between the PDGF and BDNF proteins and the methylation status of corresponding genes. Immunoblots were performed from 75µg of proteins and Actin was used as loading control. Methylation status of *PDGF* and *BDNF* gene was assessed by methylation sensitive restriction assay (MSRA).

Figure 4. Schematic representation of gliomagenesis induced by the disruption of the Dnmt1/PCNA and/or Dnmt1/UHRF1 interactions.
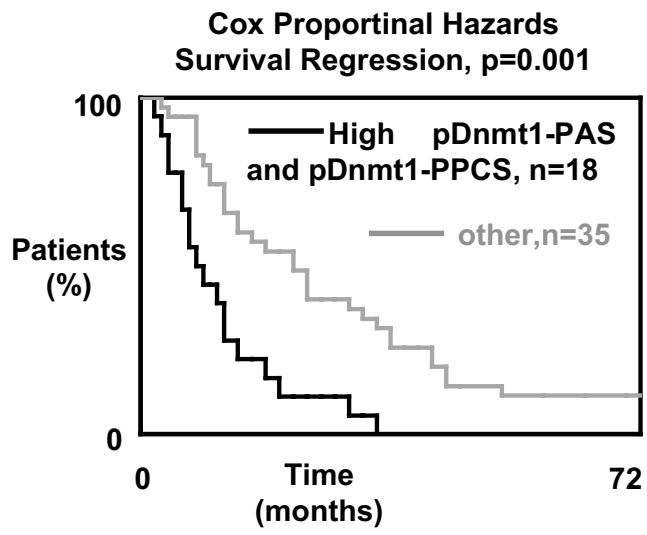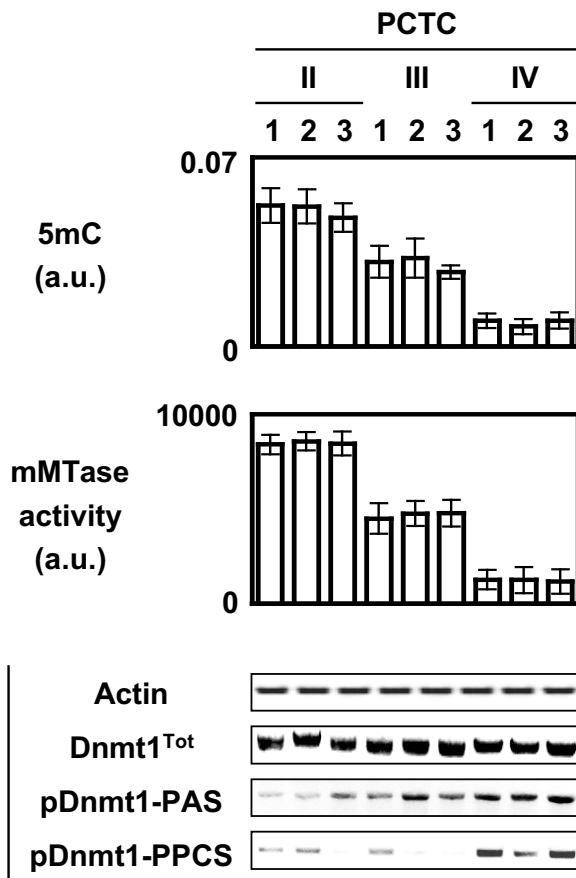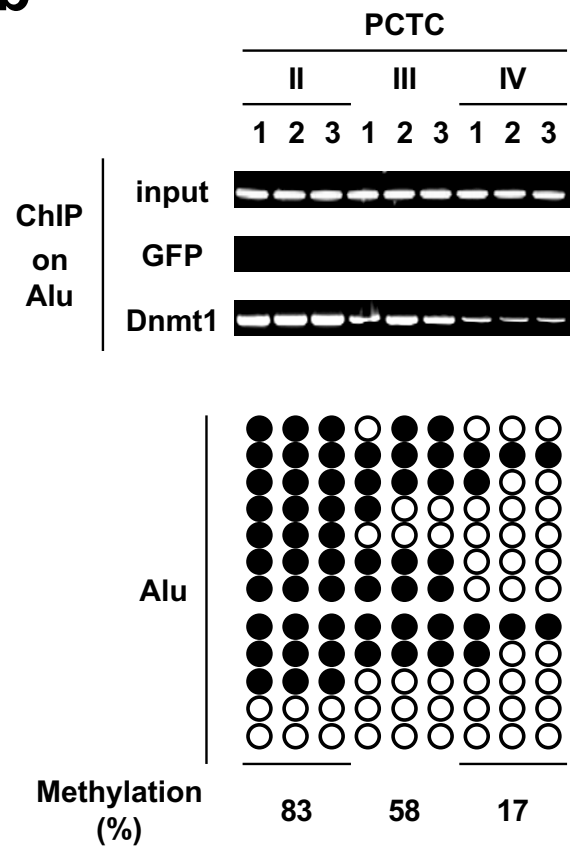
a

gliomas

nt	II	III	IV
5	16	16	30

5mC
(a.u.)

0.4

0

Pearson's correlation test
n=67, r=-0.504, p<0.0001

b

0.4

5mC
(a.u.)

0

0   dnMTase activity (a.u.)   20

Pearson's
correlation
test

n=67
r=0.135
p=0.2761

0.4

5mC
(a.u.)

0

0   mMTase activity   20
(a.u.)

n=67
r=0.760
p<0.0001

c

Pearson's correlation test
n=67, r=-0.202, p=0.1012

9

Relative
Dnmt1
Expression
(a.u.)

0

0   mMTase activity (a.u.)   20

d

3

pDnmt1-PAS
Expression
(a.u.)

0

0   20

Pearson's
correlation
test

n=67
r=-0.569
p<0.0001

0.8

pDnmt1-PPCS
Expression
(a.u.)

0

0   20

mMTase activity (a.u.)

n=67
r=-0.454
p=0.0001

figure 1

e

Cox Proportinal Hazards
Survival Regression, p=0.001

figure 1

a

PCTC

	II			III			IV		
	1	2	3	1	2	3	1	2	3

5mC (a.u.)

0.07

0

mMTase activity (a.u.)

10000

0

WB

Actin
Dnmt1^{Tot}
pDnmt1-PAS
pDnmt1-PPCS

b

PCTC

	II			III			IV		
	1	2	3	1	2	3	1	2	3

ChIP on Alu

input
GFP
Dnmt1

Alu

Methylation (%)

83   58   17

c

401-615

peptideU (596-614)

UHRF1   356-635

1   793

1-446   1081-1408

PCNA   HDAC1

peptideP   163-174   686-812

NL   CXXC   BAH1   BAH1   Catalytic domain

1   1616

S143 ← Akt

S127 ← PKC

figure 2

a

Ntv-a

| peGFP | + | - |
| peGFP-UP | - | + |

IP Dnmt1

Dnmt1

UHRF1

PCNA

5mC (a.u.)

0.5

0

t test p<0.0001

b

Ntv-a/Ras-Akt
Ntv-a/peGFP-UP
Ntv-a/PDGF
Ntv-a/peGFP

Volume (mm³)

2000

0

Time (days)

0   25

c

Ntv-a

| peGFP | + | - |
| peGFP-UP | - | + |

DEVDase activity (a.u.)

1

0

p=0.0038

Relative Ki67 expression

1

0

p=0.0026

Clonogenicity index

1

0

p=0.048

d

Ntv-a

| peGFP | + | - |
| peGFP-UP | - | + |

WB

Actin

PDGF-B

BDNF

MSRA

PDGF-B — i, D

BDNF — i, D

figure 3

figure 4